Profound effects of gastric secretion rate variations on the precipitation of erlotinib in duodenum – an *in vitro* investigation

Yiwang Guo and Changquan Calvin Sun *

Pharmaceutical Materials Science and Engineering Laboratory, Department of Pharmaceutics, College of Pharmacy, University of Minnesota, 308 Harvard St. S.E. Minneapolis, MN 55455

**Corresponding author*

Changquan Calvin Sun, Ph.D.

9-127B Weaver-Densford Hall

308 Harvard Street S.E.

Minneapolis, MN 55455

Email: sunx0053@umn.edu

Tel: 612-624-3722

Fax: 612-626-2125

Abstract

Using an artificial stomach and duodenum (ASD), we investigated the pH-dependent precipitation of erlotinib (ERL) during dissolution in the gastrointestinal (GI) tract by varying the rate of gastric fluid secretion (GFS). Results show that decreasing GFS rate from 2.5 to 0.5 mL/min leads to an increased degree of supersaturation in the duodenum fluid due to elevated pH, resulting in precipitation of ERL and a reduced area under the curve (AUC) of the concentration – time profiles from 14,000 to 3,000 (µg·min)/mL. Such a change in AUC is expected to lower the bioavailability of ERL, a BCS II drug, in patients with a low GFS. This example demonstrates the potential use of ASD as an effective tool for guiding the efficient development of robust tablet formulations by better understanding the impact of GI tract pH on the fate of drugs in the duodenal fluid.

Keywords

pH; precipitation; erlotinib HCl; artificial stomach and duodenum; biorelevant dissolution.

1. Introduction

Understanding the physical processes that a drug product encounters in the gastrointestinal (GI) tract is important, because disintegration, dissolution, precipitation and solubilization events in the GI tract directly affect the bioavailability of drugs. In fact, *in vitro* dissolution behaviors have been routinely investigated to predict *in vivo* dissolution and bioavailability to facilitate the drug development process (Wang et al., 2009).

Drug dissolution can be slowed down by several physical mechanisms, such as a change in solid forms (Alonzo et al., 2011; Hawley and Morozowich, 2010; Yamashita and Sun, 2016), drug-excipient complexation (Guo and Sun, 2021; Guo et al., 2019), and agglomeration of fine particles (Bilgili et al., 2018). The interplay between a drug and GI tract environment also plays an important role. For example, a poorly soluble weak acid may precipitate out in the acidic gastric fluid (pH 1-2) when a soluble salt is administered. A weak base may precipitate out a solution in gastric fluid when it is transferred to the intestine (pH 5-7), due to the high degree of supersaturation of the unionized form in the solution (McAllister, 2010).

Since the pH condition in human GI tract can be highly variable, depending on gender, diet habit, drug therapy, food intake, and disease state (Freedberg et al., 2014; Freire et al., 2011; Fuchs and Dressman, 2014; Hens et al., 2016; Lu et al., 2010; Russell et al., 1993; Wang et al., 2015a), the precipitation behaviors of ionizable drugs in the GI tract could be highly variable among patients. Thus, a clear understanding of the dissolution performance of such drugs in a dynamic pH environment in the GI tract is important for designing tablet products with robust biopharmaceutical performance.

Although the pH variations in the GI tract depend on the dynamic fluid transfer in the GI tract, it is not captured by the current static mono-compartment pharmacopeial dissolution systems. Therefore, an *in vitro* dissolution apparatus that mimics key physiological conditions of human GI tract is of value

(Thakore et al., 2021). Several dissolution apparatuses have been developed to mimic the GI tract, such as biphasic dissolution appratus (Mudie et al., 2012), TIM-1 (Blanquet et al., 2004; Minekus et al., 1995), BioGIT System (Kourentas et al., 2018), gastrointestinal simulator (Takeuchi et al., 2014), and artificial stomach and duodenum (Carino et al., 2006; Polster et al., 2010). Although varied in design, such as number of chambers, medium volume, and application of hallow membrane, these apparatuses were all introduced based on the realization that an *in vitro* dissolution apparatus should be more than static and mono-compartmental.

In this study, we employed an ASD (Figure 1) due to its simplicity and ease of setting up. The ASD is a multi-chamber dissolution apparatus, comprising a stomach chamber and a duodenum chamber, that can mimic liquid infusion and emptying in both chambers (Carino et al., 2006, Polster et al., 2010). If the amount of drug dissolved in the duodenum chamber is proportional to the bioavailability, the ASD has the ability to rank order bioavailability of different formulations of a given drug (Carino et al., 2006, 2010; Chen et al., 2019; Polster et al., 2010; Polster et al., 2015; Wang et al., 2018). The ASD can be controlled to mimic several key physiological events, such as gastric secretion, stomach emptying, duodenal secretion and emptying. Hence, the ASD can provide a great deal of information to facilitate the understanding of physical events in the GI tract after a drug is given orally (Polster et al., 2010; Polster et al., 2015).

It has been suggested that more than half of drug molecules contain basic groups, among which >50% are either mono-basic or di-basic (Manallack, 2009; Manallack et al., 2013). These drugs can be dissolved more in the gastric fluid but are at the risk of uncontrolled precipitation in the higher pH environment of the duodenum, which could lower their bioavailability. In this work, we investigated this phenomenon using erlotinib HCl (ERL-HCl) as a model drug. ERL has a pH-dependent solubility with a pK_a of 5.42 and solubility of 0.4 mg/mL at pH 2 and 25 °C (TARCEVA (erlotinib) [package insert]). It was recognized that antacids, proton pump inhibitors and histamine H2 receptor antagonists reduce the absorption of ERL (Aronson, 2016). The commercial oral tablet of ERL-HCl, Tarceva®, has a bioavailability of ~60% and exhibits large intra- and inter-patient variability in both peak plasma concentration and AUC. The large variability may be attributed to variable dissolution of ERL in GI tract (CDER, 2004; Leeuwen et al., 2016; Yang et al., 2017), or processes that affect the absorption and metabolism of ERL (Touma et al., 2017). In this study, we focused on elucidating the potential role of changing gastric secretion rate, and pH-sensitive precipitation in the duodenum, on the dissolution of ERL in the GI tract.

2. Materials and Methods

2.1. Materials

ERL-HCl tablets (150 mg of ERL equivalent per tablet) were prepared in the laboratory using a wet granulation process. Hydrochloric acid aqueous solution (36.5%–38%, VWR international, Eagan, MN) was ACS reagent grade. FaSSIF powder was purchased from Biorelevant.com Ltd. (London, UK).

2.2. Methods

2.2.1. In vitro dissolution in an Artificial Stomach–Duodenum (ASD)

Dissolution of ERL-HCl tablets was monitored using an ASD apparatus consisting of two jacketed beakers with temperature controlled at 37 °C using a water bath (Figure 1). This apparatus simulates stomach and duodenum by regulating the fluid flow using a programmatically controlled peristaltic Masterflex L/S Easy-Load II pump (Cole-Parmer, Vernon Hills, IL).

Parameters of ASD in this work were chosen to be consistent with those in the literature (Polster et al., 2010; Polster et al., 2015; Wang et al., 2018), which accord with typical physiological conditions in fasted state (Dressman, 1986; Kararli, 1995). In the experiments, the stomach chamber contained simulated gastric fluid (0.01M HCl, pH = 2) and the duodenum chamber contained FaSSIF (pH = 6.5). The initial volume of liquid in the stomach chamber was 250 mL (50 mL simulated gastric fluid plus 200 mL dosing liquid of DI water), which was decreased to 50 mL following a first-order emptying kinetics with a halflife of 15 min. The duodenum volume was maintained at 30 mL throughout the entire study, achieved

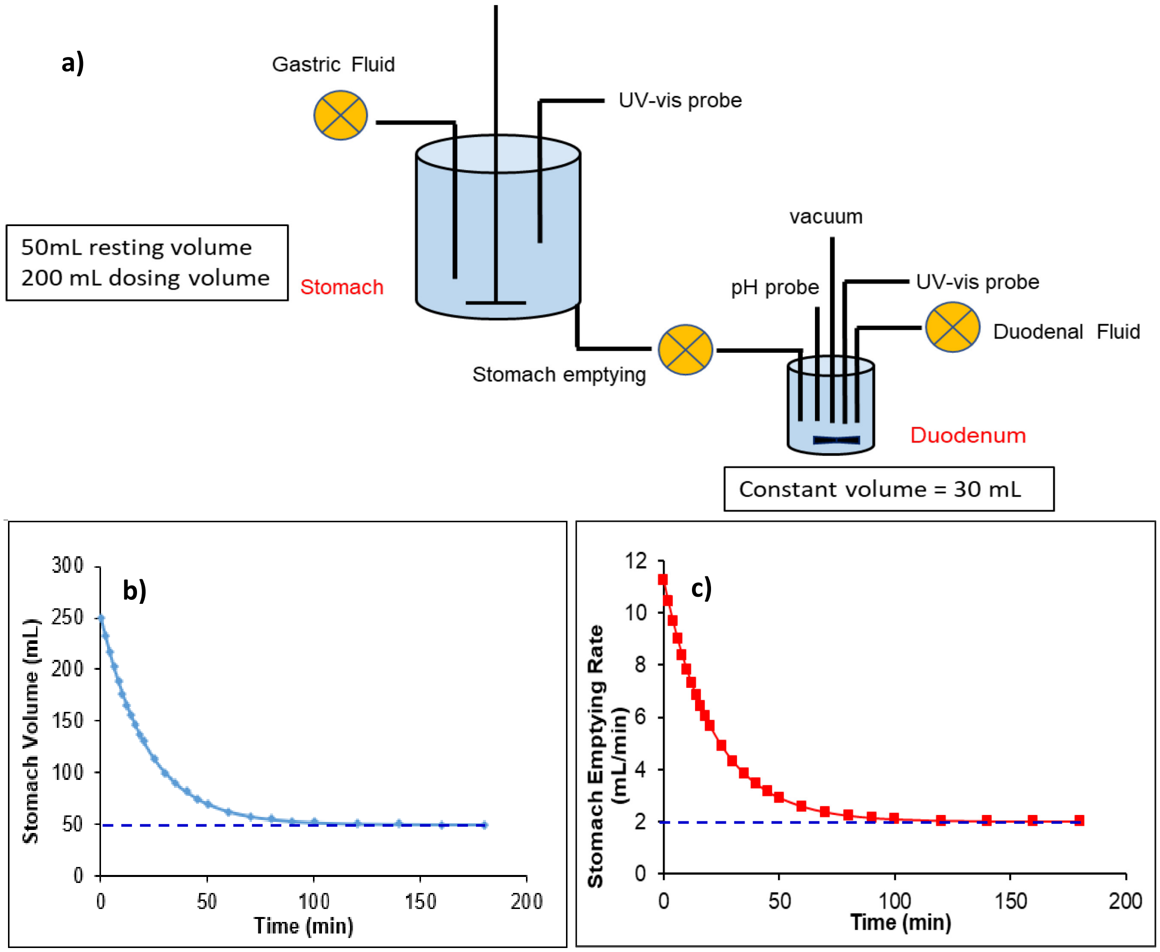

Figure 1. a) Schematic of artificial stomach and duodenum (ASD) (modified from Ref. (Wang et al., 2018)); b) Stomach fluid volume – time profile; and c) stomach emptying rate – time in ASD when the gastric secretion rate is 2 mL/min. The resting volume in the stomach chamber is 50 mL.

by setting a vacuum line in the duodenum chamber at a calibrated height. To mimic the *in vivo* secretion processes, fresh gastric fluid (0.5-2.5 mL/min) and duodenal fluid (2 mL/min) were infused into respective chambers at predetermined rates to create various pH profiles in the duodenum chamber. For a typical adult human, the gastric mucosa secretes 1.2 to 1.5 liters of gastric juice per day (Sircus, 2020), corresponding to a GSF of approximately 1 mL/min. Since pH in the GI tract can vary due to physiological reasons (Freire et al., 2011; Wang et al., 2015b), or pathophysiological reasons, such as hypochlorhydria (lack of stomach acid) or hyperchlorhydria (excessive stomach acid), the range of GSF secretion rate, 0.5 to 2.5 ml/min, was investigated in this study. The pH profile in the duodenum chamber was monitored using a pH meter (Orion Star A211, Thermo Scientific, Waltham, MA). Drug concentration was determined by a fiber optic UV/vis probe. To eliminate the interference of particles on determined concentration of ERL, a second derivative approach was used to analyze the UV absorbance data (Karpinska, 2012). Mixing was achieved by an overhead paddle stirrer (80 rpm) in the stomach chamber and a magnetic stirrer (100 rpm) in the duodenum chamber. Prior to each experiment, all pumps were calibrated. All fluids used in the experiment were degassed to avoid the generation of bubbles that might affect the UV data collection during the course of the experiment.

The area under the curve (AUC) of the concentration – time profile in the duodenum chamber was used to predict the impact of secretion rate on bioavailability, assuming that the amount of drug dissolved in duodenum chamber is proportional to bioavailability (Carino et al., 2006; Polster et al., 2010; Polster et al., 2015).

2.2.2. Simulating stomach emptying kinetics

The process of liquid transfer from stomach to duodenum follows first order kinetics, and the stomach emptying rate *R (mL/min)* is given by equation (1),

$$R = a + k(V_s - V_r) \qquad (1)$$

where *a* is the GFS rate (0.5 to 2.5 mL/min); *k* is the stomach emptying constant ($\frac{ln2}{t_{1/2}}$ = 0.04621 min^{-1}, assuming $t_{1/2}$= 15 min), V_s (*mL*) is the total volume of liquid in the stomach chamber at any given time, and V_r is the resting volume of SGF in stomach chamber (50 mL). The initial volume in the stomach chamber was 250 mL (50 mL SGF resting liquid and 200 mL DI water dosing liquid). After an ERL-HCl tablet was introduced, the stomach emptying process was initiated immediately by the programmable controlled pump to gradually lower the total volume to 50 mL (Figure 1b). The duodenum chamber receives both the secreted duodenal fluid at 2 mL/min and liquid transferred from the stomach chamber. However, the total duodenal liquid volume was maintained at 30 mL by removing excess medium using a vacuum line.

2.2.3. Nucleation induction time measurement

A pH-shift method was used to investigate the nucleation induction time, where a saturated stock solution of ERL-HCl (~0.4 mg/mL) in 0.01 M HCl was prepared. To 20 mL of this solution, different volumes of a NaOH solution (1 M) were added, resulting in solutions with different pHs. Precipitation was monitored using a fiber optic UV-Vis probe (Ocean Optics, Dunedin, FL) at 450 nm with 3 s data sampling intervals. Since ERL does not absorb UV light at this wavelength, a rise in "absorbance" is attributed to blockage of light by solid particles due to nucleation and crystal growth. Induction time was determined from the cross point between the linearly extrapolated rising portion of the curve and the baseline (Yamashita and Sun, 2019).

3. Results and Discussion

The ERL concentration – time profiles in both the stomach chamber (Figure 2a) and the duodenum chamber (Figure 3a) varied significantly with the GFS rate. The AUC of the profiles in the stomach chamber decreased approximately linearly with increasing GFS rate (Figure 2b) because of the more extensive dilution by the fresh gastric fluid and faster stomach-emptying rate (Eq. 1). On the contrary, the duodenal AUC increased with increasing GSF rate (Figure 3a). The AUC was 3,000 (µg*min)/mL at the 0.5 mL/min GFS rate but 14,000 (µg*min)/mL when GFS was greater than 2 mL/min (Figure 3b). This ~5-fold change in AUC is qualitatively correlated with the extent of precipitation in the duodenum chamber. For example, the visually observed precipitation was extensive when GFS = 0.5 mL/min, but absent when the GFS was 2 mL/min or higher. Since the amount of drug dissolved in duodenum directly impacts bioavailability, the pH sensitive precipitation behavior of ERL in the duodenum chamber was further investigated.

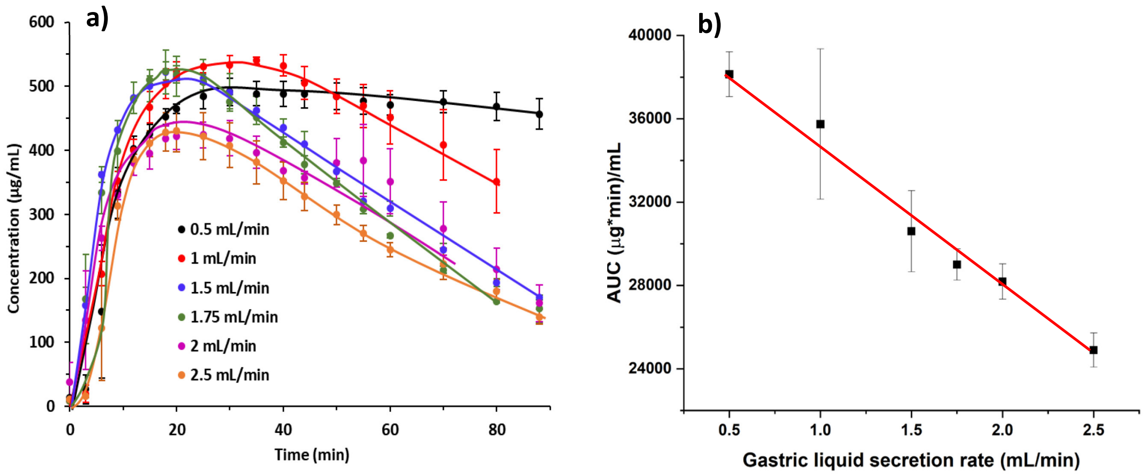

Figure 2. a) Concentration – time profiles and b) AUC of erlotinib in the stomach chamber of ASD at different gastric secretion rates (n = 3).

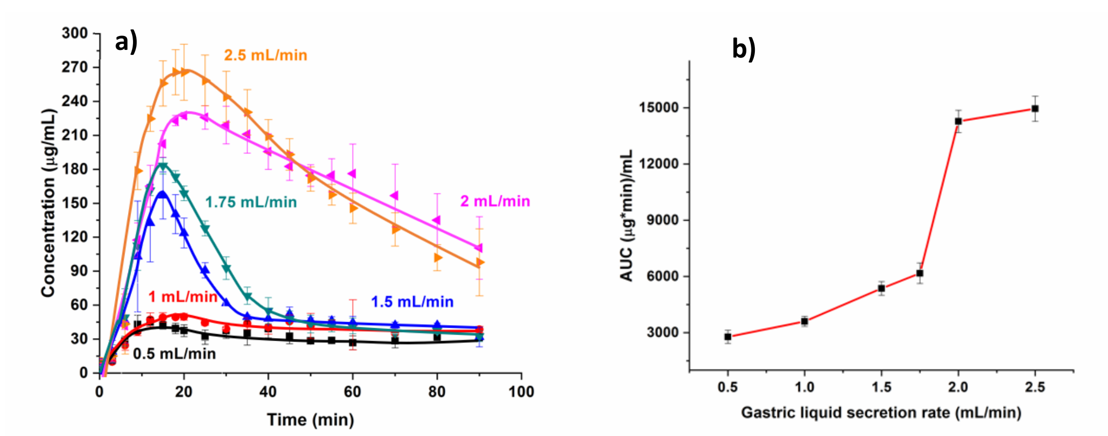

Figure 3. Effects of GFS rate on a) duodenal concentration - time profiles, and b) AUC of erlotinib in the duodenum medium (n = 3).

To explain the visually observed effect of GFS rate on the precipitation of ERL, we monitored the pH – time profile in the duodenum chamber throughout the course of experiment (Figure 4). The pH of the initial duodenual medium, i.e., FaSSIF, was 6.5. As the gastric fluid enters the duodenum chamber, the pH decreased for all groups but occurred more rapidly with a faster gastric secretion rate. For secretion rates in the range of 0.5 – 2 mL/min, the pH reached a minimum value at ~17 min before rising. The rise in pH with time was due to the continuous infusion of FaSSIF (pH = 6.5) at a rate of 2 mL/min, combined with the decreasing rate of gastric fluid transfer (Figure 1c). When the GFS rate changed from 0.5 to 2 mL/min, the pH at 90 min in the duodenal medium varied from 6.2 to 4.2. When the GFS rate was 2.5 mL/min, the pH continued to decrease after 17 min, reaching approximately 2.8 at 90 min. In this case, the volume of SGF entering the duodenum was sufficient to acidify the replenishing FaSSIF and, thereby, maintained a low pH in the duodenum medium.

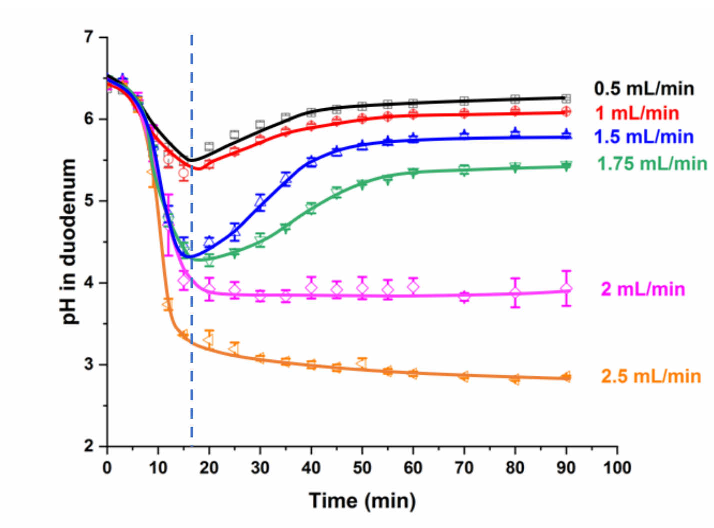

Figure 4. pH – time profiles in duodenum medium with the GSF rate varying from 0.5 to 2.5 mL/min (n =3).

In addition to monitoring the pH, we also measured the induction times of ERL precipitation in different pH media using a UV dip probe at 25 °C (Ilevbare et al., 2013) (Figure 5). The pH of an ERL solution in 0.01 M HCl (~0.4 mg/mL) was raised to different pH values by adding suitable volumes of a 1 M NaOH solution. ERL molecules in the initial HCl solution were essentially ionized since the pH was more than 3 pH units below the pK_a of ERL (= 5.42 at 25°C). While the total ERL concentration did not change significantly, the concentration of neutral ERL increased sharply with increasing pH when the solution pH passed the pK_a in accordance with the Henderson-Hasselbalch equation. Consequently, the degree of supersaturation (Eq. 2) of neutral ERL increased significantly, which led to the precipitation tendency of ERL free base differing by several orders of magnitude as measured by induction time (0 - 500 min) (Figure 5a).

$$S = \frac{C}{C_s} \tag{2}$$

where C is the total concentration of neutral ERL in a given solution and C_s is the intrinsic solubility of the ERL free base in water, which is 4.9 ± 0.9 µg/mL at 25 °C (Tóth et al., 2016).

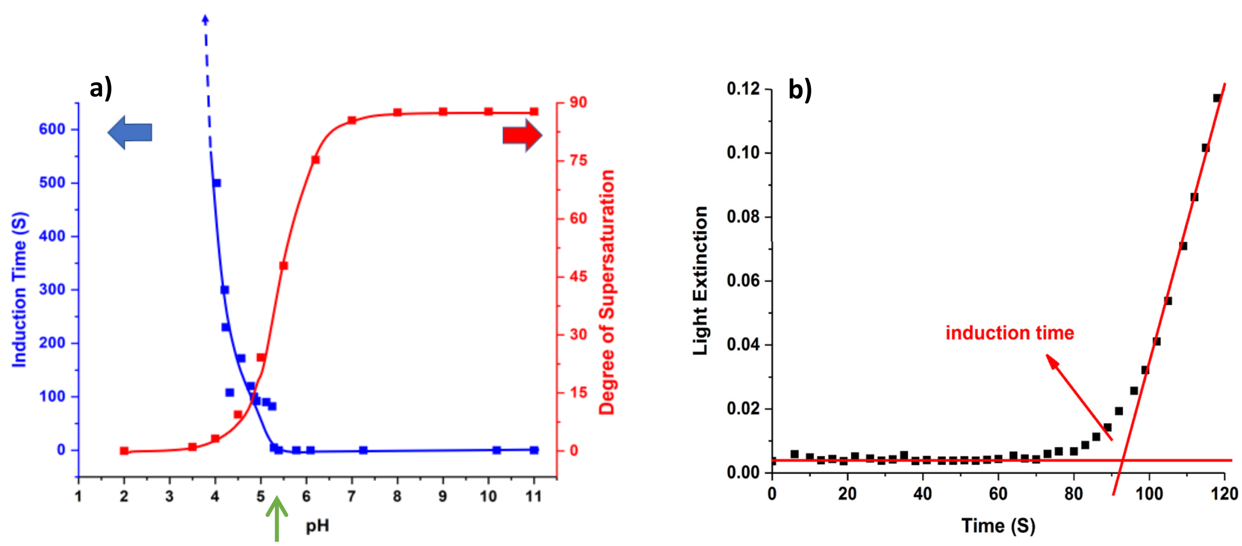

Figure 5. a) Induction time and calculated degree of supersaturation as a function of pH in duodenum (pK_a is indicated with an arrow). b) Induction time determination from UV-vis data obtained at pH 5.12.

Precipitation took place immediately when the equilibrium pH was greater than the pK_a, corresponding to an S > 40 (Figure 5a). The induction time rose sharply when equilibrium pH decreased below pK_a, reaching more than 6 h at a pH = 3.6, corresponding to S = 1.22. This explains the drastically different precipitation behaviors observed in the duodenum chamber with different solution pHs when the GFS rate was varied between 0.5 and 2.5 mL/min (Figure 4). Thus, variable GFS rates could potentially lead to substantially different amounts of drug dissolved in the duodenal fluid, resulting in a larger AUC at a faster GFS rate (Figure 3).

We chose ERL as a model drug in this work because it is a BCS class II drug (Sanphui et al., 2016), which has a high permeability and poor solubility. Because the rate limiting process to bioavailability of ERL is mainly dissolution, not permeation, in the GI tract, ERL tablets would benefit from formulation strategies that maintain robust dissolution behavior by minimizing precipitation in the duodenum even at a high duodenal pH. Useful strategies to prevent uncontrolled precipitation in the duodenum could include 1) incorporating a nucleation inhibitor in the formulation (Price et al., 2019) and 2) incorporating a pH modifier (Guo and Sun, 2022).

Various experimental attempts have also been reported to investigate the pH effect in GI tract on dissolution of ionizable drugs, including utilization of dissolution media with different pHs in the static mono-compartment USP apparatus (Zhou et al., 2005); transferring fluid at a constant rate among several chambers (Gu et al., 2005); simulating the physiological dynamic fluid transfer in multi-compartment apparatus (Bhattachar et al., 2011), mimicking the absorption process by using fiberglass dialysis (Blanquet et al., 2004), caco-2 cell membrane (Kobayashi et al., 2001), or coupling with the physiological based pharmacokinetic (PBPK) model to predict *in vivo* pharmacokinetics (Bhattachar et al., 2011; Hens and Bolger, 2019). This work demonstrates that the relatively simple ASD setup can be quite useful in understanding the impact of changes in key human GI tract physiological parameters on drug dissolution. Although this is demonstrated here using a weakly basic drug, ERL, the application of ASD can be reasonably extrapolated to other weakly ionizable BCS II drugs to efficiently screen for formulations that exhibit robust dissolution in the GI tract. Moreover, similar to the investigation of the effects of gastric secretion rate, ASD can be used to investigate the effects of many other factors, such as stomach emptying and food effect, on dissolution and precipitation of drugs. The use of duodenal AUC to rank order bioavailability of formulations is valid only if dissolution is the rate limiting step for absorption. If the absorption of a drug is limited by the permeation process, the in vitro dissolution data does not predict bioavailability. For ERL, the reduced total concentration of ERL in the duodenal fluid is accompanied by a higher percentage of neutral ERL, which is expected to exhibit a higher permeability than the ERL cation. However, the assumption that the permeation step is not rate limiting for absorption is reasonable as the interconversion between the neutral and cationic species of ERL in solution is much faster than crossing the membrane, which is high for ERL (i.e., high permeability). For other classes of drugs, the in vitro dissolution investigation may not predict bioavailability, since bioavailability is also affected by first pass effect by CYP3A4, biliary secretion into the duodenum, and GI wall secretion by P-glycoprotein. Other more sophisticated *in vitro* tools or *in silico* techniques that account for such limitations should be employed when reliable predictions of bioavailability is sought.

4. Conclusion

Using an ASD, this work shows that the profound changes in the AUC of erlotinib in duodenum is explained by pH variations in duodenum due to a change in GFS rate, which leads to the variable precipitation kinetics. This mechanism may also be applicable to other weakly basic drugs with a similar pK_a. As pH in the GI tract is variable among patients, results of such a study using ASD can provide insights and guide the efficient development of robust tablet formulations to maximize the chance of success in clinical studies.

Acknowledgements

We thank Dr. Michael Hawley for guidance with setting up the artificial stomach and duodenum apparatus. Y.G. thanks the Graduate School of the University of Minnesota for a Doctoral Dissertation Fellowship (2020 – 2021) and the Department of Pharmaceutics, University of Minnesota for a David J.W. Grant & Marilyn J. Grant Fellowship in Physical Pharmacy (2020 – 2021).

References

Alonzo, D.E., Gao, Y., Zhou, D., Mo, H., Zhang, G.G.Z., Taylor, L.S., 2011. Dissolution and Precipitation Behavior of Amorphous Solid Dispersions. *JPharm Sci,* 100, 3316-3331.

Aronson, J.K., 2016, Erlotinib in Meyler's Side Effects of Drugs, 6th Ed., pp. 97-98.

Bhattachar, S.N., Perkins, E.J., Tan, J.S., Burns, L.J., 2011. Effect of gastric pH on the pharmacokinetics of a bcs class II compound in dogs: Utilization of an artificial stomach and duodenum dissolution model and gastroplus,™ simulations to predict absorption. *J Pharm Sci* 100, 4756-4765.

Bilgili, E., Rahman, M., Palacios, D., Arevalo, F., 2018. Impact of polymers on the aggregation of wet-milled itraconazole particles and their dissolution from spray-dried nanocomposites. *Adv Powder Technol* 29, 2941-2956.

Blanquet, S., Zeijdner, E., Beyssac, E., Meunier, J.P., Denis, S., Havenaar, R., Alric, M., 2004. A dynamic artificial gastrointestinal system for studying the behavior of orally administered drug dosage forms under various physiological conditions. *Pharm. Res.* 21, 585-591.

Carino, S.R., Sperry, D.C., Hawley, M., 2006. Relative bioavailability estimation of carbamazepine crystal forms using an artificial stomach-duodenum model. *J Pharm Sci* 95, 116-125.

Carino, S.R., Sperry, D.C., Hawley, M., 2010. Relative bioavailability of three different solid forms of PNU-141659 as determined with the artificial stomach-duodenum model. *J Pharm Sci* 99, 3923-3930.

CDER, 2004. Drugs@FDA, in: Research, C.f.D.E.a. (Ed.), Washington D.C: U.S. Food and Drug Administration.

Chen, H., Guo, Y., Wang, C., Dun, J., Sun, C.C., 2019. Spherical Cocrystallization—An Enabling Technology for the Development of High Dose Direct Compression Tablets of Poorly Soluble Drugs. *Cryst. Growth Des.* 19, 2503-2510.

Dressman, J. B., 1986. Comparison of canine and human gastrointestinal physiology. *Pharma Res*. 3, 123-131.

Freedberg, D.E., Lebwohl, B., Abrams, J.A., 2014. The impact of proton pump inhibitors on the human gastrointestinal microbiome. *Clin. Lab. Med.* 34, 771-785.

Freire, A.C., Basit, A.W., Choudhary, R., Piong, C.W., Merchant, H.A., 2011. Does sex matter? The influence of gender on gastrointestinal physiology and drug delivery. *Int J Pharm* 415, 15-28.

Fuchs, A., Dressman, J.B., 2014. Composition and physicochemical properties of fasted‐state human duodenal and jejunal fluid: A critical evaluation of the available data. *J Pharm Sci* 103, 3398-3411.

Gu, C.H., Rao, D., Gandhi, R.B., Hilden, J., Raghavan, K., 2005. Using a novel multicompartment dissolution system to predict the effect of gastric pH on the oral absorption of weak bases with poor intrinsic solubility. *J Pharm Sci* 94, 199-208.

Guo, Y., Sun, C.C., 2021. Pharmaceutical Lauryl Sulfate Salts: Prevalence, Formation Rules, and Formulation Implications. *Mol Pharm*. 19, 432-439

Guo, Y., Wang, C., Dun, J., Du, L., Hawley, M., Sun, C.C., 2019. Mechanism for the Reduced Dissolution of Ritonavir Tablets by Sodium Lauryl Sulfate. *J Pharm Sci* 108, 516-524.
Hawley, M., Morozowich, W., 2010. Modifying the Diffusion Layer of Soluble Salts of Poorly Soluble Basic Drugs To Improve Dissolution Performance. *Mol Pharm* 7, 1441-1449.
Hens, B., Bolger, M.B., 2019. Application of a Dynamic Fluid and pH Model to Simulate Intraluminal and Systemic Concentrations of a Weak Base in GastroPlus(™). *J Pharm Sci* 108, 305-315.
Hens, B., Brouwers, J., Corsetti, M., Augustijns, P., 2016. Supersaturation and Precipitation of Posaconazole Upon Entry in the Upper Small Intestine in Humans. *J Pharm Sci* 105, 2677-2684.
Ilevbare, G.A., Liu, H., Edgar, K.J., Taylor, L.S., 2013. Maintaining Supersaturation in Aqueous Drug Solutions: Impact of Different Polymers on Induction Times. *Cryst. Growth Des.* 13, 740-751.
Kararli, T. T., 1995. Comparison of the gastrointestinal anatomy, physiology, and biochemistry of humans and commonly used laboratory animals. *Biopharm Drug Dispos* 16, 351-380.
Karpinska, J., 2012. Basic principles and analytical application of derivative spectrophotometry. Macro to nano spectroscopy, book edited by Jamal Uddin, 253-256.
Kobayashi, M., Sada, N., Sugawara, M., Iseki, K., Miyazaki, K., 2001. Development of a new system for prediction of drug absorption that takes into account drug dissolution and pH change in the gastro-intestinal tract. *Int J Pharm* 221, 87-94.
Kourentas, A., Vertzoni, M., Barmpatsalou, V., Augustijns, P., Beato, S., Butler, J., Holm, R., Ouwerkerk, N., Rosenberg, J., Tajiri, T., Tannergren, C., Symillides, M., Reppas, C., 2018. The BioGIT System: a Valuable In Vitro Tool to Assess the Impact of Dose and Formulation on Early Exposure to Low Solubility Drugs After Oral Administration. *AAPS J.* 20, 71.
Leeuwen, R.W.F.v., Peric, R., Hussaarts, K.G.A.M., Kienhuis, E., IJzerman, N.S., Bruijn, P.d., Leest, C.v.d., Codrington, H., Kloover, J.S., Holt, B.v.d., Aerts, J.G., Gelder, T.v., Mathijssen, R.H.J., 2016. Influence of the Acidic Beverage Cola on the Absorption of Erlotinib in Patients With Non–Small-Cell Lung Cancer. *J. Clin. Oncol.* 34, 1309-1314.
Lu, P.-J., Hsu, P.-I., Chen, C.-H., Hsiao, M., Chang, W.-C., Tseng, H.-H., Lin, K.-H., Chuah, S.-K., Chen, H.-C., 2010. Gastric juice acidity in upper gastrointestinal diseases. *World J. Gastroenterol.* 16, 5496.
Manallack, D.T., 2009. The acid-base profile of a contemporary set of drugs: implications for drug discovery. *SAR QSAR Environ Res.* 20, 611-655.
Manallack, D.T., Prankerd, R.J., Yuriev, E., Oprea, T.I., Chalmers, D.K., 2013. The significance of acid/base properties in drug discovery. *Chem Soc Rev* 42, 485-496.
McAllister, M., 2010. Dynamic Dissolution: A Step Closer to Predictive Dissolution Testing? *Mol Pharm* 7, 1374-1387.
Minekus, M., Marteau, P., Havenaar, R., Veld, J.H.J.H.i.t., 1995. A Multicompartmental Dynamic Computer-controlled Model Simulating the Stomach and Small Intestine. *Altern Lab Anim.* 23, 197-209.
Mudie, D.M., Shi, Y., Ping, H., Gao, P., Amidon, G.L., Amidon, G.E., 2012. Mechanistic analysis of solute transport in an in vitro physiological two-phase dissolution apparatus. *Biopharm Drug Dispos.* 33, 378-402.
Polster, C.S., Atassi, F., Wu, S.-J., Sperry, D.C., 2010. Use of Artificial Stomach−Duodenum Model for Investigation of Dosing Fluid Effect on Clinical Trial Variability. *Mol Pharm* 7, 1533-1538.
Polster, C.S., Wu, S.J., Gueorguieva, I., Sperry, D.C., 2015. Mechanism for enhanced absorption of a solid dispersion formulation of LY2300559 using the artificial stomach duodenum model. *Mol Pharm* 12, 1131-1140.
Price, D.J., Ditzinger, F., Koehl, N.J., Jankovic, S., Tsakiridou, G., Nair, A., Holm, R., Kuentz, M., Dressman, J.B., Saal, C., 2019. Approaches to increase mechanistic understanding and aid in the selection of precipitation inhibitors for supersaturating formulations–a PEARRL review. *J. Pharm. Pharmacol* 71, 483-509.

Russell, T.L., Berardi, R.R., Barnett, J.L., Dermentzoglou, L.C., Jarvenpaa, K.M., Schmaltz, S.P., Dressman, J.B., 1993. Upper Gastrointestinal pH in Seventy-Nine Healthy, Elderly, North American Men and Women. *Pharm Res* 10, 187-196.

Sanphui, P., Rajput, L., Gopi, S.P., Desiraju, G.R., 2016. New multi-component solid forms of anti-cancer drug Erlotinib: role of auxiliary interactions in determining a preferred conformation. *Acta Crystallogr. B: Struct. Sci. Cryst. Eng. Mater.* 72, 291-300.

Sircus, W., Dworken, . Harvey J. , Hightower, . Nicholas Carr and Keeton, . William T. , 2020. Human digestive system. Encyclopedia Britannica.

Takeuchi, S., Tsume, Y., Amidon, G.E., Amidon, G.L., 2014. Evaluation of a three compartment in vitro gastrointestinal simulator dissolution apparatus to predict *in vivo* dissolution. *J Pharm Sci* 103, 3416-3422.

TARCEVA (erlotinib) [package insert], O.P.I., Melville, NY, 2004.

Thakore, S.D., Sirvi, A., Joshi, V.C., Panigrahi, S.S., Manna, A., Singh, R., Sangamwar, A.T., Bansal, A.K., 2021. Biorelevant dissolution testing and physiologically based absorption modeling to predict in vivo performance of supersaturating drug delivery systems. *Int. J. Pharm.* 607, 120958.

Tóth, G., Jánoska, Á., Szabó, Z.-I., Völgyi, G., Orgován, G., Szente, L., Noszál, B., 2016. Physicochemical characterisation and cyclodextrin complexation of erlotinib. *Supramol. Chem* 28, 656-664.

Touma, J.A., McLachlan, A.J., Gross, A.S., 2017. The role of ethnicity in personalized dosing of small molecule tyrosine kinase inhibitors used in oncology. *Transl. Cancer Res.* S1558-S1591.

Wang, C., Chopade, S.A., Guo, Y., Early, J.T., Tang, B., Wang, E., Hillmyer, M.A., Lodge, T.P., Sun, C.C., 2018. Preparation, Characterization, and Formulation Development of Drug–Drug Protic Ionic Liquids of Diphenhydramine with Ibuprofen and Naproxen. *Mol Pharm* 15, 4190-4201.

Wang, Q., Fotaki, N., Mao, Y., 2009. Biorelevant dissolution: methodology and application in drug development. *Dissolution Technol* 16, 6-12.

Wang, Y.T., Mohammed, S.D., Farmer, A.D., Wang, D., Zarate, N., Hobson, A.R., Hellström, P.M., Semler, J.R., Kuo, B., Rao, S.S., 2015a. Regional gastrointestinal transit and pH studied in 215 healthy volunteers using the wireless motility capsule: influence of age, gender, study country and testing protocol. *Aliment. Pharmacol. Ther.* 42, 761-772.

Wang, Y.T., Mohammed, S.D., Farmer, A.D., Wang, D., Zarate, N., Hobson, A.R., Hellström, P.M., Semler, J.R., Kuo, B., Rao, S.S., Hasler, W.L., Camilleri, M., Scott, S.M., 2015b. Regional gastrointestinal transit and pH studied in 215 healthy volunteers using the wireless motility capsule: influence of age, gender, study country and testing protocol. *Aliment. Pharmacol. Ther.* 42, 761-772.

Yamashita, H., Sun, C.C., 2016. Harvesting Potential Dissolution Advantages of Soluble Cocrystals by Depressing Precipitation Using the Common Coformer Effect. *Cryst. Growth Des.* 16, 6719-6721.

Yamashita, H., Sun, C.C., 2019. Expedited Tablet Formulation Development of a Highly Soluble Carbamazepine Cocrystal Enabled by Precipitation Inhibition in Diffusion Layer. *Pharm res* 36, 90.

Yang, K.M., Shin, I.C., Park, J.W., Kim, K.S., Kim, D.K., Park, K., Kim, K., 2017. Nanoparticulation improves bioavailability of Erlotinib. *Drug Dev Ind Pharm.* 43, 1557-1565.

Zhou, R., Moench, P., Heran, C., Lu, X., Mathias, N., Faria, T.N., Wall, D.A., Hussain, M.A., Smith, R.L., Sun, D., 2005. pH-dependent dissolution in vitro and absorption in vivo of weakly basic drugs: development of a canine model. *Pharm res* 22, 188-192.